O-GlcNAcylation modification of MyoD regulates skeletal muscle fiber differentiation by antagonizing the UPF1 pathway

Received for publication, September 25, 2024, and in revised form, December 24, 2024 Published, Papers in Press, February 27, 2025,
https://doi.org/10.1016/j.jbc.2025.108364

Lele Kou[1], Meng Zhang[2], Xiaoshuang Li[1], Ziyang Zhang[1], Wenjin Guo[2], Boxi Zhang[1], Peisong Yang[1], Yuxin Xia[1], Huijie Wang[1], Bin Xu[1,*], and Shize Li[1,*]

From the [1]College of Animal Science and Veterinary Medicine, Heilongjiang Bayi Agricultural University, Heilongjiang, Daqing, China; [2]College of Animal Science and Veterinary Medicine, Jilin University, Changchun, Jilin, China

Reviewed by members of the JBC Editorial Board. Edited by Enrique De La Cruz

Skeletal muscle is an essential tissue for maintaining the body's basic functions. The basic structural unit of skeletal muscle is the muscle fiber, and its type is the main factor that determines the athletic ability of animals. The *O*-linked N-acetylglucosamine (*O*-GlcNAc) modification, a reversible protein post-translational modification, is involved in many important biological processes such as gene transcription, signal transduction, cell growth, and differentiation. Myogenic differentiation factor (MyoD), the first discovered myogenic regulatory factor, facilitates the transformation of fibroblasts into skeletal muscle cells. In early laboratory studies, MyoD was found to be modified by *O*-GlcNAcylation. However, the regulatory effects and mechanisms of *O*-GlcNAcylation modification on MyoD in skeletal muscle development and differentiation remain unclear. Therefore, our research was aimed at exploring the mechanism of MyoD in skeletal muscle differentiation under the influence of *O*-GlcNAcylation modification, through *O*-linked N-acetyl glucosamine transferase (OGT) or *O*-N-acetylaminoglucosidase manipulation, as well as MyoD supplementation. During the differentiation of C2C12 cells, *O*-GlcNAcylation of MyoD was found to be mediated by OGT, through its interaction with MyoD. Additionally, OGT was found to antagonize with up-frameshift protein 1 in inhibiting the ubiquitination-mediated degradation of MyoD *via* the K48 site, thereby regulating myotube formation. In mouse skeletal muscle tissue, *Ogt* gene deletion led to the differentiation of mouse skeletal muscle fibers from fast-twitch muscle fibers to slow-twitch muscle fibers, whereas this effect was mitigated by supplementation with exogenous MyoD. These results enhance understanding of the regulatory mechanisms of *O*-GlcNAcylation modification of MyoD in muscle development and differentiation. Our findings also indicate potential therapeutic targets for muscle and metabolism-related diseases.

Skeletal muscle consists of thousands of muscle fibers with contractile properties. Myoblasts in animals undergo proliferation and hypertrophy, thereby forming muscle fibers with multinuclear, contractile, and functional characteristics (1). The heterogeneous nature of mammalian skeletal muscle ensures flexibility; consequently, skeletal muscle can perform various types of exercise (2), such as sustained endurance exercise or high-intensity racing exercise, and rapid and strong contractions (3). The number and type of muscle fibers composing skeletal muscle are highly conserved across species. The number of muscle fibers is usually determined at birth (4–6). With continuous growth and development of the body, muscle fibers change in size and type (6). The growth and development of skeletal muscle exhibit high plasticity in response to various conditions and are regulated by a variety of complex networks (7). Myogenic regulatory factors (MRFs) (8–10) play key roles in the formation of muscle fibers and regulate the transcription of muscle-specific genes (11). This family encodes four muscle-specific transcription factors: myogenic differentiation factor (MyoD), myogenin (MyoG), myogenic factor 5 (Myf5), and myogenic regulatory factor (MRF4), also known as Myf6 or herculin (12, 13). These transcription factors regulate the proliferation and cell cycle arrest of precursor cells, activation, and differentiation of muscle-specific genes, thereby influencing the differentiation of stem cells into muscle-derived lineage cells (14). The MRFs family also regulates the level of myosin heavy chain (MyHC), which determines the contraction characteristics of muscle fibers to some extent. It has been reported that the regulatory ability of myogenic differentiation is closely related to the disease progression of sarcopenia/skeletal muscle atrophy and Duchenne muscular dystrophy (15). MyoD, the first myogenic regulator discovered in the MRF family, in 1988, leads to the conversion of fibroblasts into skeletal muscle cells (16). In early stages of skeletal muscle development, MyoD is initially expressed in the precursor cells of skeletal muscle (17) and, through interaction with other muscle-derived regulatory factors, activates the expression of muscle-specific genes, thereby facilitating muscle cell differentiation and fusion and ultimately muscle fiber formation. For example, the *MyoD* gene and *Myf5* gene cooperatively regulate the differentiation of somatic cells into myoblasts (18). Expression of the *MyoG*

* For correspondence: Shize Li, lishize@byau.edu.cn; Bin Xu, xubin@byau.edu.cn.

gene is controlled by the *MyoD* and *Myf5* genes, facilitating the differentiation of myoblasts into mature skeletal muscle cells (19). In addition, the MyoD gene promoter exhibits priming activity in C2C12 myoblasts and has been found to be specific to muscle tissue (20). MyoD also binds and targets the promoters of Mef2C and MyoG, thereby promoting the expression of muscle-specific genes and facilitating the formation of myotubes. At the same time, some studies have pointed out that inhibiting MyoD can alter the differentiation direction of fast and slow muscle fibers (21, 22). Therefore, MyoD plays a crucial role in skeletal muscle development.

The *O*-linked N-acetylglucosamine (*O*-GlcNAc) modification is a post-translational protein modification involved in cell signal transduction. In glucose metabolism, approximately 2% to 5% of glucose enters the hexosamine biosynthetic pathway. UDP-N-acetyl glucosamine (23), generated through the action of glutamine-fructose-6-phosphoamidotransfrase, participates in the synthesis of secretory glycoproteins and membrane structure glycoproteins. Simultaneously, UDP-N-acetyl glucosamine serves as the substrate for *O*-linked N-acetyl glucosamine transferase (OGT). N-Acetylglucosamine (GlcNAc), a product of the hexosamine biosynthetic pathway, is linked to serine or threonine residues in proteins through a β-configuration *O*-glycosidic bond. The entire process is mediated by OGT and *O*-N-acetylaminoglucosidase (OGA) (24). OGT-mediated signal transduction is a necessary process for normal skeletal muscle metabolism and systemic energy balance (25). In addition, OGT regulates muscle phenotype through IL-15 and interferes with the OGT-IL-15 nutrition sensing axis, thus offering a new approach to combat obesity and metabolic disorders (26). Liu Y*et al.* have found that *O*-GlcNAcylation contributes to reversing metabolic disorders, stress, and cell death in skeletal muscle (27). Studies have shown that *O*-GlcNAcylation occurs as C2C12 myoblasts differentiate into myotubes and regulates various protein interactions (28). Ogawa *et al.* (29) has discovered that *O*-GlcNAcylation levels significantly decrease during myogenic differentiation. Moreover, after inhibition of OGA activity with Thiamet G, the activity of MyoG and Mrf4 is inhibited. Relevant muscle-specific genes, such as MyHC and troponin, in C2C12, are also affected by OGA inactivation (29). In a mouse model with skeletal muscle–specific knockout (KO) of the *Ogt* gene, significantly diminished skeletal muscle quality, elevated numbers of mitochondria, and diminished fat content have been observed (25). These findings suggest that *O*-GlcNAcylation modification plays a crucial role in skeletal muscle development.

At present, the specific mechanism of MyoD regulates skeletal muscle development has not been fully elucidated. Additionally, the relationship between MyoD and O-GlcNAcylation, as well as their effects on skeletal muscle development and differentiation are still unclear. Therefore, the purpose of this study was to elucidate the mechanism through which *O*-GlcNAcylation of MyoD regulates skeletal muscle development and differentiation in mice. The study was aimed at identifying potential targets and strategies for more precise, comprehensive, and accurate regulation of skeletal muscle development in the future.

Results

O-GlcNAcylation modification regulates myoblast differentiation in vitro

We transfected C2C12 cells with lentivirus for overexpression of OGT (Fig. S1*A*). Subsequently, *Ogt* gene and protein expression (Fig. 1*A* and *D*) and overall *O*-GlcNAcylation modification (Fig. 1*D*) increased significantly, thus suggesting successful construction of the OGT overexpression model. Myoblast differentiation requires a variety of transcription factors and differentiation factors. MyoD was used as a differentiation marker; myosin heavy chain 2 (Myh2) and myosin heavy chain 4 (Myh4) were selected as fast muscle fiber markers; and myosin heavy chain 7 (Myh7) was used as a slow muscle fiber marker. The upregulation of MyoD was associated with increased *O*-GlcNAcylation (Fig. 1, *B* and *E*); moreover, Myh2 and Myh4 increased significantly, while Myh7 decreased (Fig. 1, *C* and *E*). Subsequently, we performed transfection with OGT knockdown lentivirus. The decrease in OGT expression (Fig. 1*F*) significantly decreased MyoD (Fig. 1, *G* and *J*) and overall *O*-GlcNAcylation modification (Fig. 1*I*); moreover, Myh2 and Myh4 decreased, whereas Myh7 significantly increased (Fig. 1, *H* and *J*). Immunofluorescence results further confirmed these findings (Fig. 1, *K*–*N*). In addition, the fusion index of cells transfected with lentivirus and differentiated for 3 days was significantly higher in the knockdown group than in the control group (Fig. S1, *B* and *C*). These results indicated that inhibiting *O*-GlcNAcylation modification can promote the formation of myotubes in C2C12 cells.

To investigate the effects of *O*-GlcNAcylation on C2C12 myoblasts, we treated C2C12 cells with the OGT inhibitor OSMI-1, at a final concentration of 100 μM, and the OGA inhibitor Thiamet G, at a final concentration of 20 μM. The treatments were performed for 24 h and 6 h, respectively, to stimulate cell differentiation over a period of 3 days. Under the action of OSMI-1, the mRNA expression of *MyoD* (Fig. 2*B*), *Myh2*, and *Myh4* decreased significantly, whereas the mRNA expression of *Myh7* increased significantly (Fig. 2*C*). Simultaneously, overall *O*-GlcNAcylation levels decreased significantly, as did the protein expression of MyoD, Myh2, and Myh4. In contrast, the expression of Myh7 increased significantly (Fig. 2*D*). The expression of genes and proteins after Thiamet G treatment had exactly the reverse result (Fig. 2, *E*–*H*). These findings suggested that *O*-GlcNAcylation regulates the myogenic differentiation of C2C12 cells.

MyoD is glycosylated by O-GlcNAc and relies on OGT enzymatic activity

To verify whether MyoD is glycosylated with *O*-GlcNAc, we conducted immunoprecipitation tandem mass spectrometry to enrich all proteins interacting with OGT in C2C12 cells. This screening indicated an interaction between OGT and MyoD (Fig. 3*A*). Therefore, we co-expressed Flag-OGT [wildtype(WT)] and HA-MyoD (WT) plasmids in C2C12 cells. Co-precipitation demonstrated that MyoD co-expressed with OGT was strongly glycosylated (Fig. 3*B*). Subsequently, externally verified 293T cells were used for

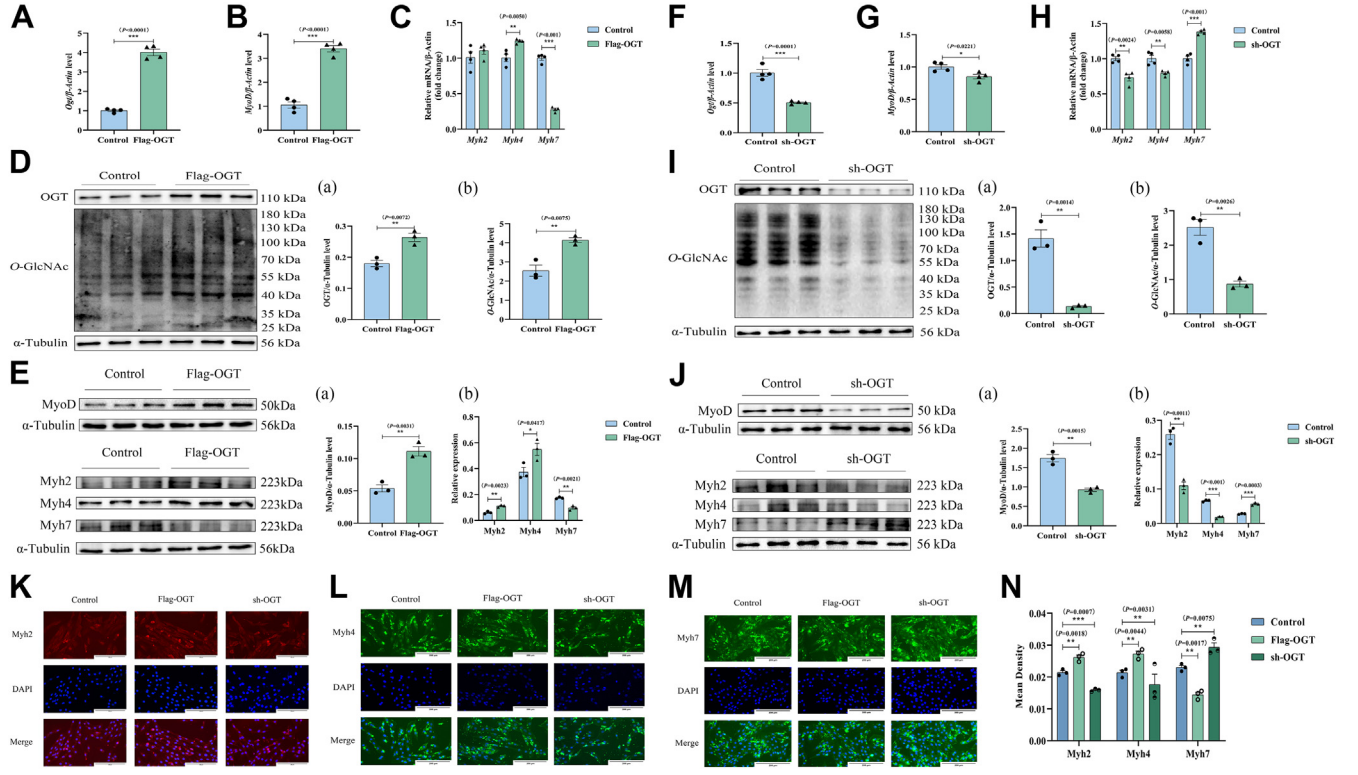

Figure 1. *O*-GlcNAcylation modification regulates the myoblast differentiation process. *A–C,* RT-qPCR method was employed to analyze the gene expression of *Ogt*, *MyoD*, and myosin subtypes following the addition of Flag-OGT. *D–E,* Western blot analysis was performed to detect the expression of OGT, *O*-GlcNAc, MyoD, and myosin subtypes following the addition of Flag-OGT. a and b, the analysis diagram of Western blot. *F–H*, RT-qPCR method was used to detect the gene expression of *Ogt*, *MyoD*, and myosin subtypes after adding sh-OGT. *I–J*, Western blot was used to detect the expression of OGT, MyoD, and myosin subtypes after adding sh-OGT. a and b, the analysis diagram of Western blot. *K–N,* immunofluorescence method was employed to detect Myh2 (*red*), Myh4 (*green*), and Myh7 (*green*) in C2C12 myoblasts, and the scale was 200 μm. The data are means ± s. d. (n = 3/4). *$p < 0.05$, **$p < 0.01$, and ***$p < 0.001$ as determined by using a *t* test. Myh2, myosin heavy chain 2; Myh4, myosin heavy chain 4; Myh7, myosin heavy chain 7; MyoD, myogenic differentiation factor; OGA, *O*-linked N-acetylaminoglucosidase; *O*-GlcNAc, *O*-linked N-acetylglucosamine; OGT, *O*-linked N-acetyl glucosamine transfer.

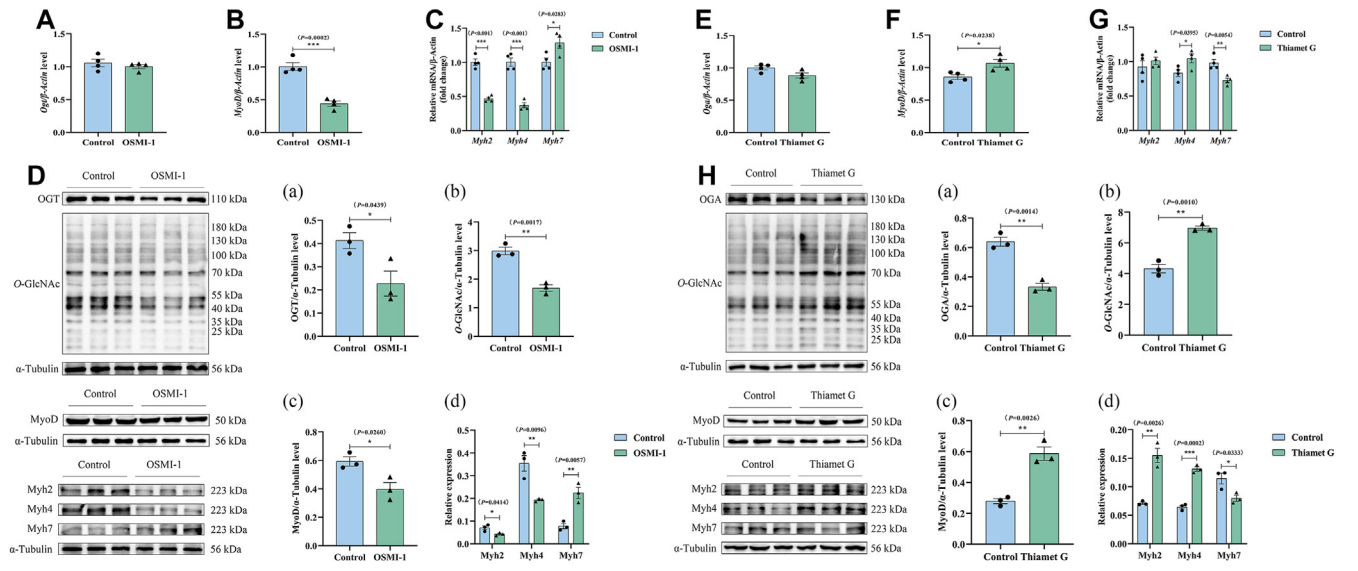

Figure 2. Inhibition or enhancement of *O*-GlcNAcylation modification can regulate the myoblast differentiation process. *A–C*, RT-qPCR method was used to detect the gene expression of *Ogt*, MyoD, and myosin subtypes after the addition of OSMI-1. *D*, Western blot was utilized to detect the expression of OGT, *O*-GlcNAc, MyoD, and myosin subtypes after the addition of OSMI-1. a–d, the analysis diagram of Western blot. *E–G,* RT-qPCR method was used to detect the gene expression of *Ogt*, MyoD, and myosin subtypes after adding Thiamet G; *H*, Western blot was used to detect the expression of OGT, *O*-GlcNAc, MyoD, and myosin subtypes after adding Thiamet G. a–d, the analysis diagram of Western blot. The data are means ± s. d. (n = 3/4). *$p < 0.05$, **$p < 0.01$, ***$p < 0.001$ as determined by using a *t* test. Myh2, myosin heavy chain 2; Myh4, myosin heavy chain 4; Myh7, myosin heavy chain 7; MyoD, myogenic differentiation factor; OGA, *O*-linked N-acetylaminoglucosidase; *O*-GlcNAc, *O*-linked N-acetylglucosamine; OGT, *O*-linked N-acetyl glucosamine transfer.

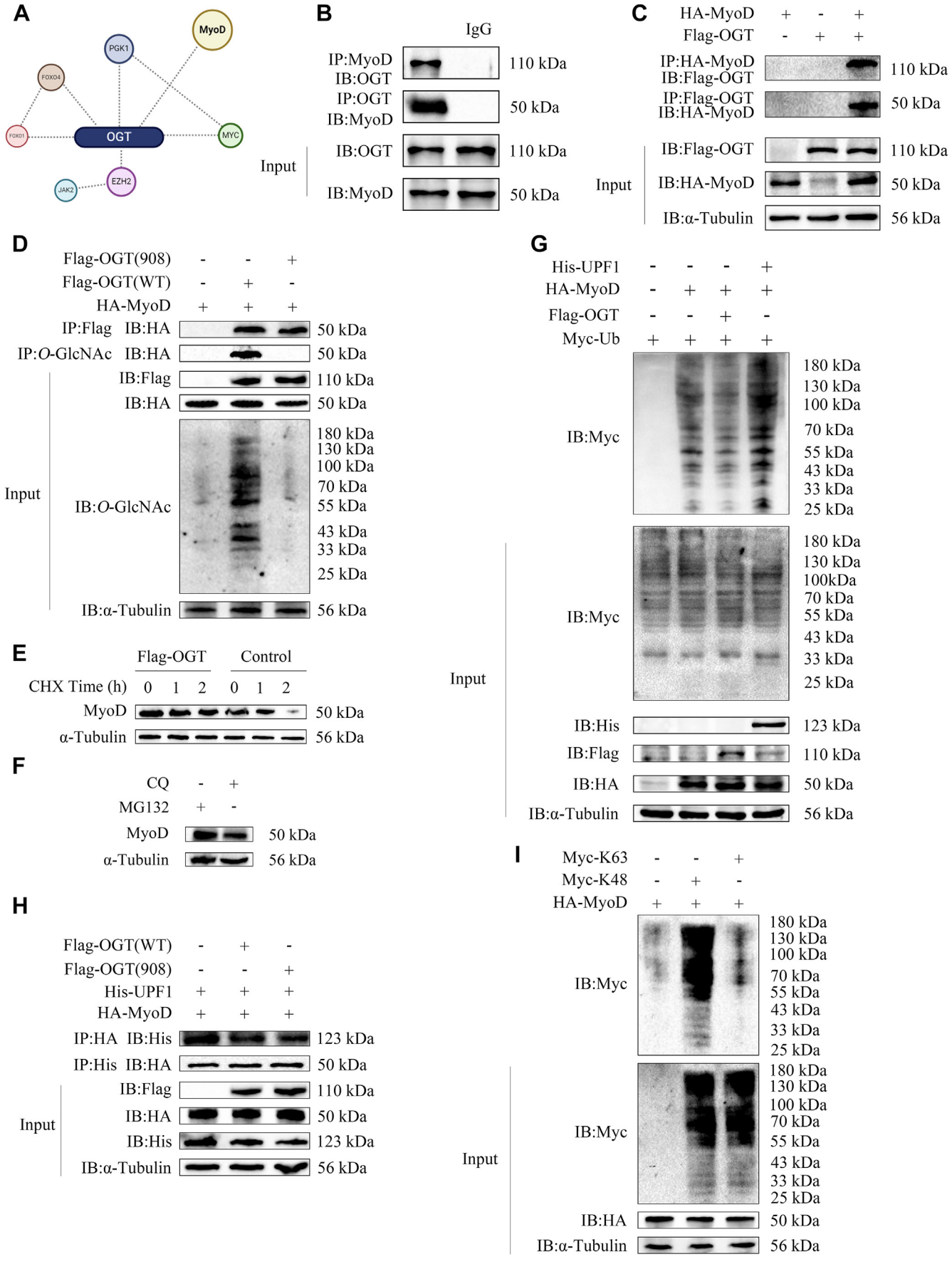

Figure 3. OGT antagonizes with UPF1 to suppress the ubiquitination degradation pathway of MyoD *via* the K48 site of MyoD. *A*, LC-MS/MS detection of proteins interacting with OGT in C2C12 cells. *B*, Co-IP method was used to detect the endogenous interaction between OGT and MyoD. *C*,

pulldown experiments (Fig. 3*C*), which indicated that MyoD was indeed glycosylated with *O*-GlcNAc. OGT's active site was located at K908 (30). When lysine at position 908 was mutated to alanine, the enzymatic activity of OGT was lost, but its protein expression level remained unaffected. To determine whether the enzymatic activity of OGT affected *O*-GlcNAcylation of MyoD, we mutated the lysine at position 908 in OGT to alanine and constructed a plasmid for ablation of OGT enzymatic activity. Co-expression of Flag-OGT (WT), Flag-OGT (908), and HA-MyoD (WT) in 293T cells indicated that OGT still interacted with MyoD after loss of enzymatic activity but did not induce *O*-GlcNAcylation of MyoD (Fig. 3*D*). This finding indicated that *O*-GlcNAcylation of MyoD is dependent on the enzymatic activity of OGT.

OGT antagonizes UPF1 to inhibit the ubiquitination degradation of MyoD

Our preliminary laboratory results suggested that *O*-GlcNAcylation modification of MyoD, in a manner dependent on OGT enzymatic activity, negatively regulates the ubiquitination-mediated degradation of MyoD in cells. We verified the ubiquitination and degradation of MyoD. First, we added the protein synthesis inhibitor cycloheximide (CHX) at a concentration of 300 μg/ml to inhibit the protein synthesis pathway. The results indicated that the protein expression of MyoD continued to decline; however, this decline was significantly inhibited following the exogenous addition of OGT (Fig. 3*E*). After administering CQ at 50 μg/ml or MG132 at 20 μg/ml to inhibit the autophagy and ubiquitination degradation pathways, we observed that the protein expression of MyoD in the CQ group was significantly lower compared to the MG132 group (Fig. 3*F*). This finding suggests that MyoD is degraded primarily through the ubiquitination pathway. Studies have suggested that the RNA decay factor up-frameshift protein 1 (UPF1) degrades MyoD protein through its E3 ligase activity (31). Therefore, we verified the co-expression of HA-MyoD, Flag-OGT, His-UPF1, and ubiquitin. *O*-GlcNAcylation indeed inhibited the ubiquitination-mediated degradation of MyoD, and UPF1 can promote the ubiquitination-mediated degradation of MyoD (Fig. 3*G*). We next sought to determine whether the relationship between OGT and UPF1 might be competitive or cooperative. Co-expression of MyoD with OGT (WT) instead of OGT (908) consistently reduced the MyoD-UPF1 interaction (Fig. 3*H*). Subsequently, we identified the proteasome degradation site, on the basis of observations that this inhibition was mediated through the K48 site (Fig. 3*I*). OGT antagonized UPF1 in inhibiting the ubiquitination-mediated degradation of MyoD, and this degradation pathway was completed *via* the K48 site of MyoD.

MyoD regulates the differentiation direction of myoblasts in the presence of O*-GlcNAcylation modification*

Studies have indicated that inhibition of MyoD expression leads to the differentiation of fast muscle fibers into slow muscle fibers (21). Therefore, we asked whether muscle fiber differentiation might change with increased MyoD expression, and how muscle fibers might differentiate if MyoD is overexpressed while the *O*-GlcNAcylation modification hydrolase is inhibited. We first transfected the HA-MyoD plasmid into C2C12 cells, then induced cell differentiation for 3 days with the OGA inhibitor Thiamet G. MyoD gene and protein expression was significantly greater in the MyoD overexpression group than the control group (Fig. 4, *B* and *F*). Additionally, addition of Thiamet G decreased the expression of OGA (Fig. 4*A*) and enhanced *O*-GlcNAcylation modification (Fig. 4*F*). Subsequently, we detected the effects of MyoD on the differentiation of C2C12 myoblasts under inhibition of the *O*-GlcNAcylation modification hydrolase, after which *O*-GlcNAcylation modification increased, and the expression of Myh2 and Myh4 significantly increased (Fig. 4, *C*, *D* and *F*), while the expression of Myh7 significantly decreased (Fig. 4, *E* and *F*). With overexpression of MyoD, expression of Myh7 decreased, while that of Myh2 and Myh4 increased. Immunofluorescence further confirmed these findings (Fig. 4, *G–J*). The results demonstrated that overexpression of MyoD accelerated the differentiation of slow muscle fibers into fast muscle fibers under inhibition of the *O*-GlcNAcylation modification hydrolase. In the absence of *O*-GlcNAcylation modification transferase, overexpression of MyoD yielded opposite results (Fig. S2, *A* and *B*). These findings suggested that overexpression of MyoD disrupts the differentiation direction of muscle fiber types in the presence of *O*-GlcNAcylation modification.

Deletion of Ogt *decreases* O*-GlcNAcylation of MyoD, thus altering the development and differentiation direction of skeletal muscle fibers in mice*

To further verify our hypothesis, we generated C57BL/6 mice with skeletal muscle-specific *Ogt* gene KO by using the Cre-loxP system (Fig. 5*A*) and intramuscularly injected MyoD recombinant lentivirus into 10-week-old mice. MyoD expression was significantly greater in the injected mice than the control mice (Fig. 5, *B* and *C*, *E* and *F*). The expression of *Ogt* in the skeletal muscle, as well as *O*-GlcNAcylation modification, was significantly diminished in the *Ogt* KO mice (Fig. 5, *D* and *F*). These results indicated that the OGT gene was successfully knocked out in the skeletal muscle in the mice. As expected, *O*-GlcNAcylation modification decreased, thus leading to a noticeable decrease in the tissue morphology of mouse gastrocnemius (Fig. S3*A*). Additionally, during the rest of the day, the respiratory entropy and oxygen consumption of

pulldown method was used to detect the exogenous interaction between OGT and MyoD. *D*, pulldown method was used to detect the *O*-GlcNAc glycosylation modification of MyoD by OGT enzyme activity. *E*, detection of MyoD stability by CHX. *F*, detection of MyoD degradation pathway by MG132 and CQ. *G*, pulldown method was used to detect the regulatory effect of OGT and UPF1 on MyoD ubiquitination. *H*, pulldown method to detect the relationship between OGT and UPF1. *I*, pulldown method was used to detect the ubiquitination site of MyoD. MyoD, myogenic differentiation factor; OGT, *O*-linked N-acetyl glucosamine transfer; UPF1, up-frameshift protein 1; CHX, cycloheximide.

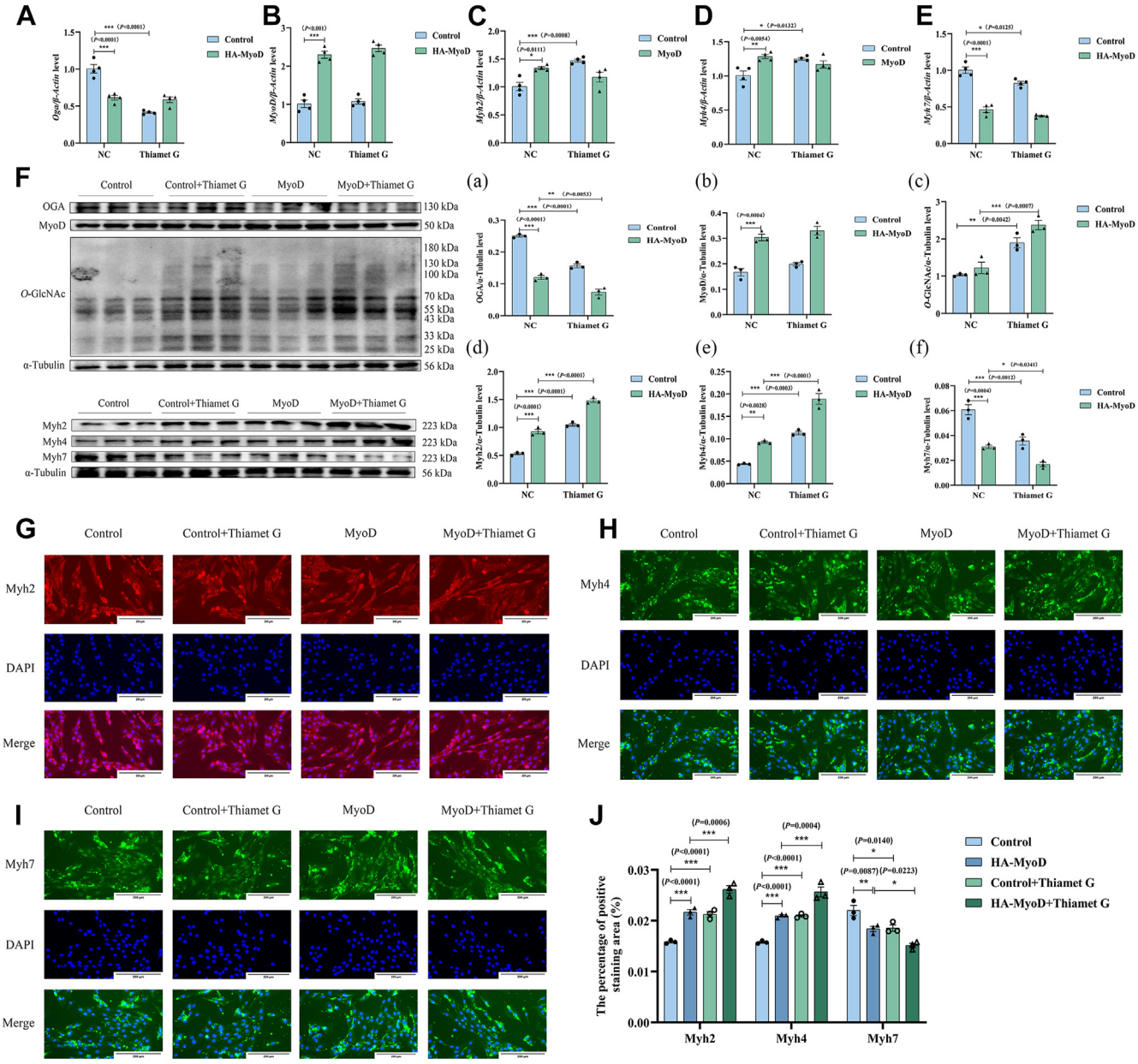

Figure 4. Inhibition of OGA and overexpressing MyoD can regulate the type of MyHC in the myogenic differentiation of C2C12 cells. *A–E*, RT-qPCR method was used to detect the gene expression of different subtypes of *Oga*, *MyoD*, and myosin. *F*, Western blot method was used to detect the expression of various protein subtypes, including OGA, MyoD, *O*-GlcNAc, and myosin. a–f, the analysis diagram of Western blot. *G–J*, the expression of Myh2 (*red*), Myh4 (*green*), and Myh7 (*green*) in C2C12 myoblasts was detected by immunofluorescence, and the scale was 200 μm. The data are means ± s. d. (n = 3/4). $*p < 0.05$, $**p < 0.01$, $***p < 0.001$ as determined by using a two-way ANOVA. Myh2, myosin heavy chain 2; Myh4, myosin heavy chain 4; Myh7, myosin heavy chain 7; MyoD, myogenic differentiation factor; OGA, *O*-linked N-acetylaminoglucosidase; *O*-GlcNAc, *O*-linked N-acetylglucosamine; OGT, *O*-linked N-acetyl glucosamine transfer.

mice increased significantly. The energy metabolism of mice was disordered, suggesting that *Ogt* KO mice require more exercise to regulate the energy balance in their bodies (Fig. S3, *B–G*). In addition, the results of ATPase staining showed an increase in the proportion of type I muscle fibers (light staining) and a decrease in the proportion of type II muscle fibers (intense staining). After overexpression of MyoD, the proportion of type I and type II muscle fibers recovered (Fig. 5, *G* and *H*). Simultaneously, the expression of Myh2 and Myh4 in *Ogt* KO mice decreased significantly (Fig. 5, *I* and *J* and *L*), while the expression of Myh7 increased significantly (Fig. 5, *K* and *L*). After injection of lentivirus, the expression of fast and slow muscles recovered. The tissue immunofluorescence results were also consistent with these findings (Fig. 5, *M* and *N*). Our results demonstrated that *Ogt* deletion induced the differentiation of muscle fibers from fast-twitch to slow-twitch, whereas overexpression of MyoD counteracted this effect. With the increase in slow muscle fibers, the level of oxidative phosphorylation in the body was significantly altered, thus suggesting that mitochondria, the primary sites of oxidative phosphorylation, might have been affected. We subsequently examined the gastrocnemius mitochondria in mice and

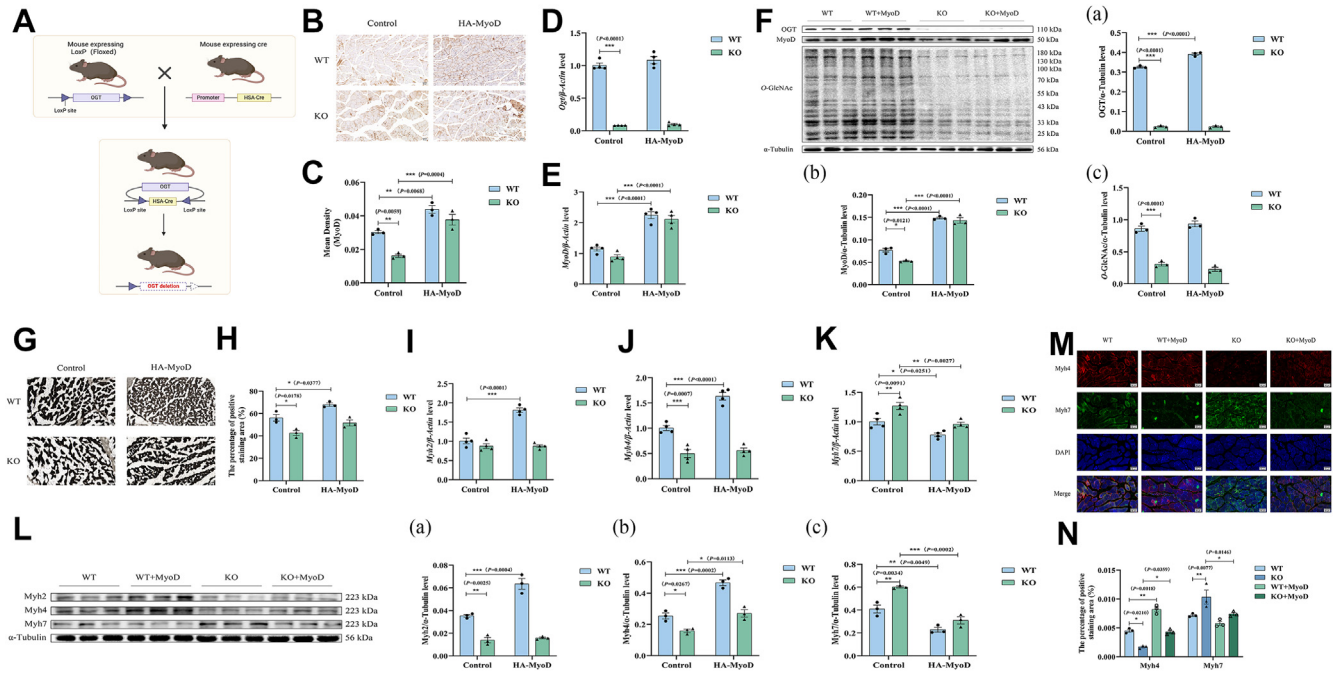

Figure 5. MyoD regulates the development and differentiation of skeletal muscle fibers in *Ogt*-deficient mice. *A*, breeding scheme involving mice with a specific knockout of the *Ogt* gene (*Ogt* KO) and wildtype control (WT). *B–C*, immunohistochemical results of mouse gastrocnemius muscle. *D*, RT-qPCR method was used to detect the gene expression of *Ogt*. *E*, RT-qPCR method was used to detect the gene expression of MyoD. *F*, Western blot was used to detect the protein expression of OGT, MyoD, and *O*-GlcNAc. a–c, the analysis diagram of Western blot. *G–H*, ATPase staining results of mouse gastrocnemius muscle tissue. *I–K*, RT-qPCR method was utilized to detect the gene expression of various myosin subtypes. *L*, Western blot analysis was employed to detect the expression of different myosin subtypes. a–c, the analysis diagram of Western blot. *M–N*, the expression of Myh4 (*red*) and Myh7 (*green*) in mouse gastrocnemius was identified through immunofluorescence, with a scale of 50 μm. The data are means ± s. d. (n = 3/4). *$p < 0.05$, **$p < 0.01$, ***$p < 0.001$ as determined by using a two-way ANOVA. Myh2, myosin heavy chain 2; Myh4, myosin heavy chain 4; Myh7, myosin heavy chain 7; MyoD, myogenic differentiation factor; OGA, *O*-linked N-acetylaminoglucosidase; *O*-GlcNAc, *O*-linked N-acetylglucosamine; OGT, *O*-linked N-acetyl glucosamine transfer; WT, wildtype; KO, knockout.

observed significantly diminished basic oxygen consumption, reserve respiratory capacity, ATP production capacity, and maximum respiratory capacity of the mitochondria in the gastrocnemius tissue in the KO group (Fig. S3, *H* and *I*). These findings were also observed in the mice in the KO group after MyoD overexpression (Fig. S3, *J* and *K*). Simultaneously, the mitochondria in the gastrocnemius tissue in the KO group swelled to varying degrees. Part of the outer mitochondrial membrane dissolved, and the mitochondrial ridge fracture disappeared. These effects were slightly alleviated after the injection of lentivirus (Fig. S3*L*). Deletion of the *Ogt* gene therefore damaged the mitochondrial function of skeletal muscle in mice.

Discussion

The differences in the development and differentiation of various types of muscle fibers underscore their distinct clinical significance in different muscle-related diseases. Consequently, finding effective ways to intervene in the differentiation of various muscle types to meet market demands has become a primary focus. In this study, *O*-GlcNAcylation was found to regulate MyoD differentiation in skeletal muscle. In C2C12 myoblasts, the status of *O*-GlcNAcylation changed, thus interfering with the differentiation of fast and slow muscle fibers in C2C12 myoblasts. In mice, deletion of the *Ogt* gene led to muscle shrinkage, mitochondrial damage, and a change in the direction of muscle fiber differentiation. These effects were somewhat alleviated by overexpression of MyoD. We discovered that MyoD undergoes *O*-GlcNAcylation modification. Additionally, we observed that OGT antagonizes UPF1 in preventing the ubiquitination-mediated degradation of MyoD at the K48 site. These findings suggest that MyoD might be a potential target for the treatment of skeletal muscle–related diseases resulting from *O*-GlcNAcylation modification.

Studies increasingly indicate that *O*-GlcNAcylation participates in numerous biological processes (32). Some studies have suggested that *O*-GlcNAcylation is closely associated with the regulation of skeletal muscle development. Skeletal muscle is the primary target organ of insulin, and nutrition-driven *O*-GlcNAcylation is the key regulator of skeletal muscle insulin signal transduction (33). C2C12 myoblasts are precursor cells of skeletal muscle with strong proliferation and differentiation ability. Ogawa *et al.* (29) has found that *O*-GlcNAcylation levels significantly decrease during myogenic differentiation, in agreement with previous research conducted by the laboratory team. During myogenic differentiation, *O*-GlcNAc levels decreased as the number of myogenic differentiation days increased. On this basis, lentiviral OGT overexpression and knockdown revealed that increased *O*-GlcNAcylation modification significantly decreased the level of the type I muscle fiber marker Myh7 but increased the levels of the type II a muscle fiber marker Myh2 and type II b muscle fiber marker Myh4, thereby indicating a differentiation of slow muscle

fibers into fast muscle fibers. The direction of muscle fiber type differentiation was completely reversed after *O*-GlcNAcylation modification was decreased. Addition of the OGT inhibitor OSMI-1 and the OGA inhibitor Thiamet G had comparable results, which were consistent with the findings reported by Shi H *et al.* (25). During the development of skeletal muscle, MyoD gradually exits the cell cycle, leading to a corresponding decrease in protein expression. Our results also demonstrated that *O*-GlcNAcylation modification was found to positively regulate the expression of MyoD, a myogenic regulator with key roles in regulating skeletal muscle differentiation. Therefore, we speculated that *O*-GlcNAcylation modification might serve as a target for regulating C2C12 myoblast differentiation. Indeed, an interaction between MyoD and OGT was identified through immune-combined mass spectrometry analysis and pulldown assays. According to Clarke's research (30) on the mechanism and specific structure of OGT, mutation of amino acid K908 in OGT to alanine results in a loss of enzymatic activity. Moreover, *O*-GlcNAcylation of MyoD depends on the enzymatic activity of OGT. Previous studies have demonstrated that *O*-GlcNAcylation modification can be used as a crucial regulator of autophagy, influencing autophagic flux and the fusion of autophagosomes with lysosomes (34). Concurrently, numerous studies have indicated that *O*-GlcNAcylation modification affects the stability, degradation rate, and even the proteasome activity of proteins (35, 36). Ubiquitin modification plays a vital role in the localization, metabolism, regulation, and degradation of proteins (37, 38). K48 polyubiquitination typically leads to proteasomal degradation, whereas K63 polyubiquitination modification is associated with various other cellular processes (39). By examining the ubiquitination site of MyoD, it was discovered that OGT can inhibit its ubiquitin-mediated degradation through the K48 site of MyoD. In addition, Feng *et al.* (31) has shown that the RNA helicase UPF1 can be used as an E3 ligase to impede human skeletal muscle differentiation. UPF1 inhibits MyoD protein in a proteasome-dependent manner and exhibits E3 ligase activity that targets MyoD protein degradation; as confirmed by our experimental results, OGT can inhibit the degradation of MyoD protein, while UPF1 can promote its degradation. Additionally, OGT antagonizes with UPF1 in inhibiting the MyoD ubiquitination-mediated degradation pathway through the K48 site of MyoD.

Ogawa *et al.* (29) have shown that inhibition of OGA activity with Thiamet G leads to inhibition of MyoG and Mrf4 activity, and the corresponding muscle-specific genes, such as MyHC and troponin, are also affected by OGA inactivation. After OGA knockdown by Thiamet G, slow muscle fibers decreased, and fast muscle fibers increased. These findings indicated that OGA inactivation causes slow muscle fibers to differentiate into fast muscle fibers in C2C12 myoblasts. Previous results have demonstrated *O*-GlcNAcylation modification of MyoD. We further investigated the effects of MyoD overexpression on myogenic differentiation of C2C12 under inhibition of the *O*-GlcNAcylation modification hydrolase OGA. This weakening of OGA influenced the rate at which MyoD overexpression regulated the differentiation of C2C12 myoblasts, thus accelerating the differentiation of slow muscle fibers into fast muscle fibers. In contrast, overexpression of MyoD alleviated abnormal muscle differentiation when OGT inhibitors were used to decrease *O*-GlcNAcylation modification.

Subsequently, we conducted experiments in mice with *Ogt* gene deletion to further verify these findings. Staining of tissue sections and quantitative analysis of markers of fast and slow muscle fibers indicated that *Ogt* gene deletion affected the fast and slow muscle fiber types in mouse skeletal muscle. The fast muscle fibers differentiate into slow muscle fibers, in agreement with findings reported by Shi H *et al.* (25). In addition, the gastrocnemius tissue morphology of *Ogt* gene deletion mice was significantly reduced, leading to muscular atrophy. The respiratory entropy of mice increased notably during daytime rest, indicating disordered energy metabolism. Mice with specific skeletal muscle deficiency required more exercise during the day to regulate the body's energy balance. This contrasts with the reduced heat output of *Ogt* gene deletion mice with liver-specific deficiency at night and the increased RER level (40), suggesting that specific skeletal muscle deficiency impacts muscle quality and disrupts the balance of energy metabolism. Moreover, studies have suggested that fast muscle fibers differentiate into slow muscle fibers after inhibition of MyoD expression in mice (21). Du *et al.* (22) have found that dietary betaine supplementation in mice increases muscle mass, promotes muscle formation, and alters the proportion of skeletal muscle fiber types *in vivo*, in a manner associated with MyoD. Therefore, after deletion of the *Ogt* gene, we increased the expression of MyoD through injection of MyoD overexpression lentivirus. Subsequently, the expression of Myh7 in the mouse gastrocnemius decreased while the expression of Myh4 increased. This finding contrasted with the expression pattern of fast and slow muscle fibers observed in mice after *Ogt* deletion. These results demonstrated that overexpression of MyoD effectively mitigates the alterations in muscle fiber type differentiation induced by *Ogt* deletion and gradually restores the balance between fast and slow muscle fibers. The alteration of slow muscle fibers will impact the oxidative phosphorylation level. Our examination of gastrocnemius mitochondria revealed that *Ogt* deletion notably decreases the basal oxygen consumption, ATP production capacity, and maximum respiratory capacity of mitochondria in mouse gastrocnemius tissue. Additionally, the overexpression of MyoD mitigates the mitochondrial swelling and disappearance of mitochondrial crests induced by *Ogt* deletion. This indicates that the deletion of the *Ogt* gene impairs the mitochondrial function of mouse skeletal muscle. Therefore, it is concluded that *Ogt* deletion can damage the mitochondrial function of skeletal muscle in mice, leading to changes in the oxidative phosphorylation level of the body, causing muscle fibers to differentiate from fast-twitch muscle fibers to slow-twitch muscle fibers, whereas overexpression of MyoD reverses this phenomenon.

In summary, our experimental results demonstrated that during the differentiation of C2C12 myoblasts, OGT mediates *O*-GlcNAcylation of MyoD through interaction with MyoD. Simultaneously, OGT antagonizes with UPF1 in

preventing ubiquitination-mediated degradation *via* the K48 site of MyoD, thereby regulating myotube formation. In mouse skeletal muscle tissue, deletion of the *Ogt* gene leads to a shift from fast to slow mouse skeletal muscle fibers. Furthermore, external supplementation with MyoD mitigates this effect. The detailed molecular mechanism is shown in Fig. 6. These findings provide a theoretical foundation for understanding the mechanisms of skeletal muscle metabolic changes induced by *O*-GlcNAcylation of MyoD. Furthermore, they suggest a potential target for treating skeletal muscle metabolic diseases.

Experimental procedures

Cell culture

C2C12 myoblasts were purchased from Fenghui Biological Company. Dulbecco's Modified Eagle Medium (DMEM) high-sugar medium containing 10% fetal bovine serum (C0235, Gibco) and 1% penicillin/streptomycin solution was used and cultured in a cell incubator at 37 °C with 5% CO_2. When the cell growth density reached 70% to 80%, the medium was replaced with DMEM high-glucose medium containing 2% horse serum (BL209 A, Biosharp) and 1% penicillin/streptomycin solution to induce the differentiation of C2C12 myoblasts.

Animal and muscle collection

$HSA^{+/+}$-$OGT^{LoxP/Y}$ and $HSA^{Cre/+}$-$OGT^{LoxP/Y}$ mice were purchased from Jackson Laboratory (B6.129-Ogttm1Gwh/J) in the United States. The strain of mice was C57BL/6J. Breeding was conducted according to the established scheme. Following genotype identification, KO male mice and WT male mice from the same litter were chosen as the control group for the experiment. Mice were kept in an IVC rat house, where the indoor temperature was maintained at 22 °C ± 1 °C, the indoor humidity was kept at 70% ± 10%, and the indoor light cycle was set for 12 h on and 12 h off. After the mice reached 12 weeks of age and their weights were recorded, they were euthanized. Muscle samples were then collected for histological analysis or immediately frozen in liquid nitrogen and stored at −80 °C for real-time fluorescence quantitative PCR (RT-qPCR) and protein blot analysis. All procedures are approved by the Animal Protection and Use Committee of Heilongjiang Bayi Agricultural University (DWKJXY2022067).

MyoD overexpression lentivirus injection

Ten-week-old WT and KO mice were selected and injected with a MyoD overexpression lentivirus with a titer of 2.9×10^8 TU/ml using the three-point method. The injection dose

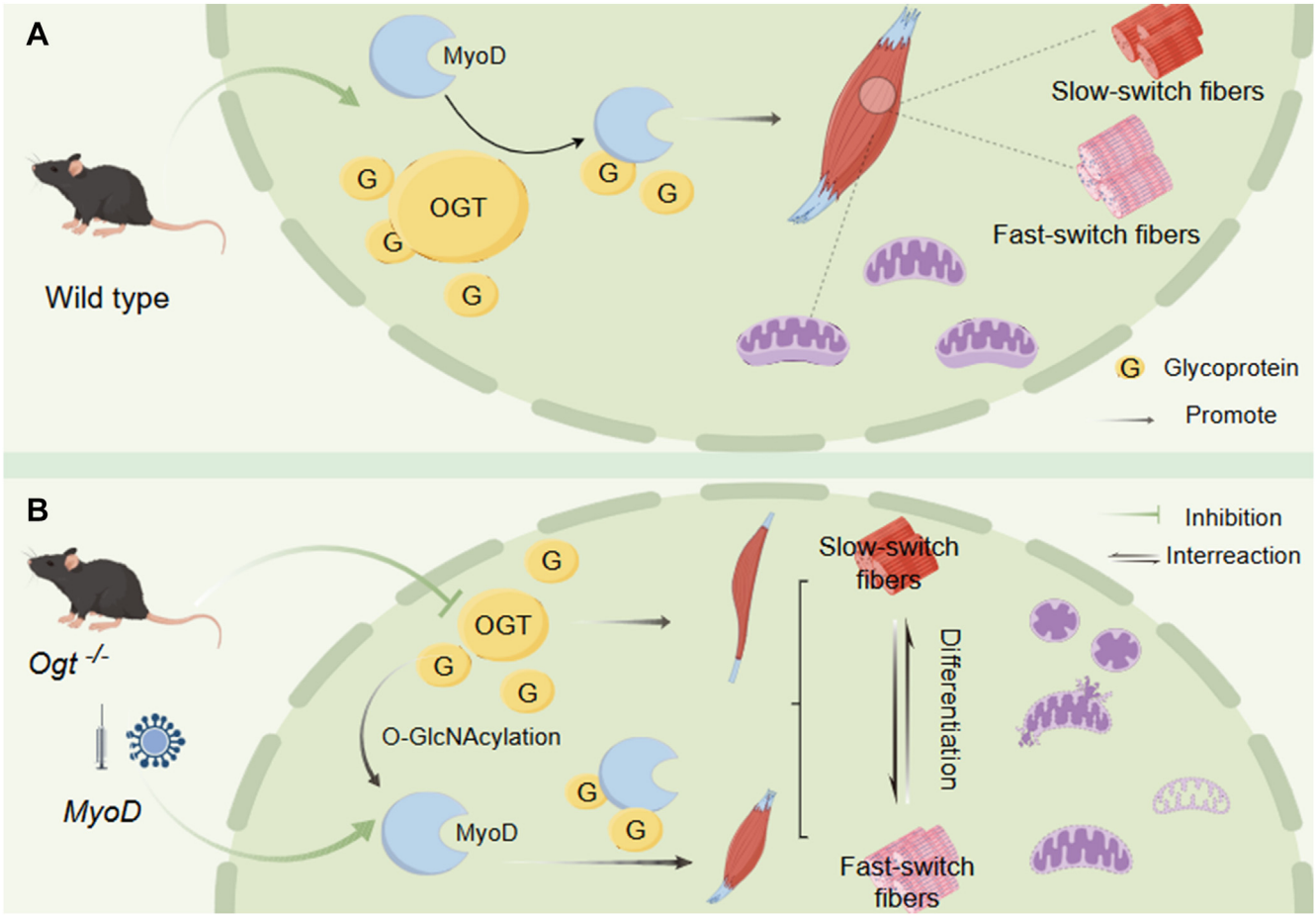

Figure 6. Mechanism of *O*-GlcNAcylation modification of MyoD in regulating skeletal muscle fiber differentiation. *A*, Wild type mice. *B*, *Ogt gene* deficient mice. MyoD, myogenic differentiation factor; OGT, *O*-linked N-acetyl glucosamine transfer.

administered was 60 μl. The mice in the injection group were labeled as HA-MyoD. The behavior and mental state of mice were observed after injection. The mice were euthanized 2 weeks later, and samples were collected.

Lentivirus transfection

Pre-experiment: Cells were inoculated into 96-well plates at a density of 3 to 5 × 10^3 cells/well. The lentivirus concentration was diluted to 1 × 10^8 TU/ml and 1 × 10^7 TU/ml using DMEM the following day and then added to the cells. The culture plates were wrapped with tin foil and placed in a cell incubator for 12 h, after which the liquid was replaced. After being infected with lentivirus for 72 to 96 h, the infection efficiency was observed using a fluorescence microscope, and the medium was changed based on the cell growth.

Formal experiment: Cells were inoculated into a 25 T-cell bottle at a rate of 1.5 to 2.5 × 10^4 cells per bottle. The lentivirus concentration was diluted to 1 × 10^8 TU/ml using DMEM the following day and then added to the cells. During this period, the liquid was changed regularly, and the cell samples were collected after 96 h of infection.

Cell transfection

Cells were inoculated into 6 cm plates at a density of 1 × 10^6 cells/well. Transfection was carried out after the cell density reached 70%. First, the culture medium in the Petri dish was replaced with 4 ml of complete culture medium. Then, a clean sterilized EP tube was taken, and 250 μl of DMEM, 5 μg of DNA, and 8 μl of Lipo8 000 transfection reagent were added to the Petri dish after thorough mixing. Wrap the Petri dish with tin foil and return it to the incubator for further culturing for 48 to 72 h, during which the liquid is typically replaced.

MyoD and Thiamet G treatment

To investigate the impact of MyoD overexpression on the differentiation of C2C12 myoblasts, the cells were transfected with the HA-MyoD plasmid when they reached 70% confluence in a 12-well plate. Subsequently, the cells were switched to a complete medium after 24 h. In order to assess the impact of MyoD on cell differentiation under *O*-GlcNAcylation modification, Thiamet G was added at a final concentration of 20 μM for 6 h. The cells were then collected on the third day of cell differentiation induction for further experiments.

Cellular immunofluorescence

The HA-MyoD plasmid was transfected, treated with 20 μM Thiamet G, induced into myogenic differentiation for 3 days, and then fixed with paraformaldehyde at room temperature for 60 min. Use a buffer to clean the residual formaldehyde, add 0.25% Triton X-100 (1139, Bio Froxx), incubate for 15 min at room temperature, and rinse with the buffer three times for 5 min each time. Add 5% skimmed milk powder and let it sit at room temperature for 1 h. Remove the milk powder and rinse with buffer solution three times, for 5 min each time. Adding antibodies for Myh2, Myh4, and Myh7 diluted in 1 × PBST and incubating at 4 °C overnight. Take it out the next day and let it stand at room temperature for 30 min. Rinse it with a buffer solution three times, for 5 min each time. Add the corresponding fluorescent rabbit/mouse antibody, incubate for 1 h at room temperature in the dark, and rinse with a buffer solution three times for 5 min each time. Finally, the anti-fluorescence quencher containing DAPI (P0131, Beyotime) was applied and observed under a fluorescence microscope.

Myoblast fusion index

According to the formula for calculating the fusion index (41, 42), the fusion index (%) = (number of nuclei in myotubes)/(total number of nuclei) × 100%. C2C12 myoblasts were cultured in DMEM until they reached a density of 80%. The cells that differentiated by the third day were stained with MYHC (ab37484, Abcam), fluorescence, and both the number of nuclei and the fusion index were calculated.

RNA extraction and real-time fluorescence quantitative PCR

Total RNA in tissues and cells was extracted using Trizol reagent. Subsequently, reverse transcription was carried out following the instructions provided by the Prime Script II first strand cDNA Synthesis Kit (RR047 A, TaKaRa) to generate cDNA. RT-qPCR was performed on the Bio-Rad IQ5 system using the SYBR Premix Ex Taq Kit (RR420 A, TaKaRa). The relative expression level of the target mRNA was calculated using the $2^{\Delta\Delta Ct}$ method. Relative expression levels of each gene were normalized to β-actin as the endogenous control for all experiments. The primers used in this study were as follows: *Ogt*-forward-primer: 5′-AGCTGTGTGTATGGAG.

TAGAGGA-3′; *Ogt*-reverse-primer: 5′-CAACAAGAAAAG TCACCAAACTGTG-3′; *Oga*-forward-primer: 5′-CCTGTTC TACCTTCCTTACGAG-3′; *Oga*-reverse-primer: 5′-TGCA-CACATCTCTTCAAACTTG-3′; *MyoD*-forward-primer: 5′-GGCTCTCTC.

TGCTCCTTTGA-3′; *MyoD*-reverse-primer: 5′-GTAGGGA AGTGTGCGTGCTC-3′; *Myh7*-forward-primer: 5′-GAATGG CAAGACGGTGACTGTG-3′; *Myh7*-reverse-

primer: 5′-GGAAGCGTAGCGCTCCTTGAG-3′; *Myh4*-forward-primer: 5′-TGATC.

ACCACCAACCCAT-3′; *Myh4*-reverse-primer: 5′-CAGCC TTGTCAGCAACTTC-3′; *Myh2*-forward-primer: 5′-ATGAG CTCCGACGCCGAG-3′; *Myh2*-reverse-primer: 5′-TCTGTTA GCATGAACTGGTAGGCG-3′; *β-Actin*-forward-primer: 5′-T ATGCTC.

TCCCTCACGCCATC-3′; *β-Actin*-reverse-primer: 5′-GTC ACGCACGATTTCCCTC.

TCAG-3′.

Western blot

According to the instructions provided by the reagent supplier, proteins were extracted from mouse C2C12 cells and mouse muscle tissues using lysis buffer (NP40/RIPA, with 1% PMSF added). The supernatant was then quantified using a BCA protein detection kit (P0010, Biyuntian) following the manufacturer's instructions and subsequently heated in

reducing SDS sample buffer. Separated by SDS-PAGE gel with the corresponding proportions and transferred to a polyvinylidene fluoride membrane (0.45 microns, 0000147800, Millipore). The membrane was sealed in Tris-buffered saline (1 × TBST) containing 5% skimmed milk powder for 1 h. It was then incubated with the appropriate primary antibody at 4 °C overnight. Subsequently, the membrane was washed in 1 × TBST and incubated with the suitable secondary antibody. The primary antibody and the secondary antibody were diluted with 1 × TBST according to the instructions, developed using ECL protein blot detection reagent (NCM Biotech), and the intensity of the band was analyzed using Image Lab software. The antibodies against OGT (1:1 000, ab96718, Abcam), OGA (1:1 000, Ab124807, Abcam), *O*-GlcNAc (1:1 000, #9875, Cell Signaling Technology), Myh2 (1:5 000, 66212-1-Ig, Proteintech), Myh4 (1:600, 20140-1-Ig, Proteintech), Myh7 (1:500, 22280-1-Ig, Proteintech), Alpha Tubulin (1:5 000, 11224-1-AP, Proteintech), and all secondary antibodies (1:10,000, SA00001–1/2, Proteintech)were also used. All antibodies are used according to the manufacturer's instructions. All uncut versions of protein profiles are documented in the source data file and supplementary information file.

Co-IP

Extract the total protein, take 500 μg of the total protein, add 4 μg of the target antibody to it, and place it in a refrigerator at 4 °C overnight to allow complete formation of the antigen–antibody complex. On the second day, firstly, 25 μg A/G magnetic beads were extracted and cleaned with 500 μl 1 × TBST. After cleaning, magnetic frames were used to separate the magnetic beads from the waste liquid. The magnetic beads were added to the antigen–antibody complex and incubated for 1 h at room temperature. After the magnetic beads are fully combined with the antigen–antibody complex, they are separated using a magnetic rack, and the supernatant is carefully aspirated. Use 1 × TBST to clean the antigen–antibody complex remaining on the magnetic beads. Subsequently, employ the buffer elution method by adding 1 × protein loading buffer to the magnetic beads. Let it stand for 10 min and then utilize a magnetic frame to separate the magnetic beads from the buffer. Finally, the magnetic beads are discarded and heated to ensure that the obtained sample is fully denatured in terms of protein. Used for subsequent experiments.

Protein ubiquitination

His-UPF1 was cotransfected with HA-MyoD and other plasmids into 293T cells. Forty-eight hours after transfection, the protein interacting with the target protein in the cell was enriched using the immunoprecipitation method. The enriched protein was then incubated with a ubiquitination antibody, followed by protein blot analysis.

Detection of protein stability using CHX

After cell pretreatment, 300 μg/ml of CHX was added, and total protein from the cells was collected at 0, 1, and 2 h, respectively. The expression of MyoD protein was then detected.

Detection of the degradation pathway of protein by CQ and MG132

After pretreatment, 50 μg/ml CQ and 20 μg/ml of MG132 were added to the cells. The total protein was collected after 2 h of treatment, and the expression of MyoD protein was subsequently detected.

Tissue immunofluorescence, immunohistochemistry, and ATPase staining

In short, the gastrocnemius tissue of mice was extracted and rapidly frozen with liquid nitrogen. The sample was cut into sagittal slices with a thickness of 30 μm using an ultramicrotome. The tissue slices were washed with PBS, sealed at room temperature, and then incubated with antibodies. After that, they were observed under a microscope. Muscle fiber types were measured using ATPase staining. Slow muscle fibers are dyed light, while fast muscle fibers are dyed dark.

Statistical analysis of data

All the data were analyzed using GraphPad Prism 8.0 software and are presented as mean ± standard deviation (SD). T-tests and two-way ANOVA were conducted among different treatment groups to determine statistical significance ($^{*}p < 0.05$; $^{**}p < 0.01$).

Data availability

The raw data that support the findings of this study are available from the corresponding author upon reasonable request.

Supporting information—This article contains supporting information.

Acknowledgments—We would like to express our gratitude to all the authors whose work has been cited here. Additionally, we extend our appreciation to the developers at Figdraw and BioRender for providing the platform used to create our figures at Figdraw.com. and BioRender.com.

Author contributions—L. K., M. Z., S. L., and B. X. conceptualization; L. K. data curation; L. K., X. L., Z. Z., and W.G. formal analysis; L. K., M. Z., X. L., Y. X., B. Z., and P. Y. investigation; L. K., Z. Y., P. Y., Y. X., and H. W. methodology; L. K., S. L., and B. X. project administration; L. K. resources; L. K., X. L., and Z. Z. software; L. K. supervision; L. K. and M. Z. validation; L. K. visualization; L. K. writing–original draft; S. L. and B. X. funding acquisition, L. K., S. L., and B. X. writing—review & editing.

Funding and additional information—This work was supported by the Biological Breeding-Major Projects in National Science and Technology (2023ZD0404606–1), National Natural Science Foundation of China (Grant No. 31972637), and National Natural Science Foundation of China (32402846).

Conflict of interest—The authors declare that they have no conflicts of interest with the contents of this article.

Abbreviations—The abbreviations used are: MRF4, myogenic regulatory factor 4; MRFs, myogenic regulatory factors; Myf5, myogenic factor 5; Myh2, myosin heavy chain 2; Myh4, myosin heavy chain 4; Myh7, myosin heavy chain 7; MyoD, myogenic differentiation factor; MyoG, myogenin; OGA, *O*-linked N-acetylaminoglucosidase; *O*-GlcNAc, *O*-linked N-acetylglucosamine; OGT, *O*-linked N-acetyl glucosamine transfer; UPF1, up-frameshift protein 1; WT, wildtype.

References

1. Cai, C., Yue, Y., and Yue, B. (2023) Single-cell RNA sequencing in skeletal muscle developmental biology. *Biomed. Pharmacother.* **162**, 114631
2. Schiaffino, S., and Reggiani, C. (2011) Fiber types in mammalian skeletal muscles. *Physiol. Rev.* **91**, 1447–1531
3. Bottinelli, R. (2001) Functional heterogeneity of mammalian single muscle fibres: do myosin isoforms tell the whole story? *Pflugers Archiv.* **443**, 6–17
4. Zheng, R. Q., and Zhang, M. (1998) Gene transplantation and progressive muscular dystrophy. *China J. Eugenics Genet.* **4**, 126–128
5. Song, S. Z., Gao, L. S., Li, H., Gong, X. Y., Liu, L. S., and Wei, Y. B. (2022) Effects of feeding levels on muscle tissue structure and muscle fiber composition related genes in sheep. *China Agric. Sci.* **55**, 4304–4314
6. Wang, T. (2019) *GPR91 Mediates Succinic Acid Regulation of Skeletal Muscleoxidative Metabolism*, South China Agricultural University. Ma.D. thesis
7. Zhang, X., Chen, M., Liu, X., Zhang, L., Ding, X., Guo, Y., *et al.* (2020) A novel lncRNA, lnc403, involved in bovine skeletal muscle myogenesis by mediating KRAS/Myf6. *Gene* **751**, 144706
8. Zhong, T., Jin, P. F., Dong, E. N., Li, L., Wang, L. J., and Zhang, H. P. (2013) Caprine sex affects skeletal muscle profile and MRFs expression during postnatal development. *Anim. Sci.* **84**, 442–448
9. Zanou, N., and Gailly, P. (2013) Skeletal muscle hypertrophy and regeneration: interplay between the myogenic regulatory factors (MRFs) and insulin-like growth factors (IGFs) pathways. *Cell Mol. Life Sci.* **70**, 4117–4130
10. Chen, W., Xu, H., Chen, X., Liu, Z., Zhang, W., and Xia, D. (2016) Functional and activity analysis of cattle UCP3 promoter with MRFs-related factors. *Int. J. Mol. Sci.* **17**, 682
11. Buckingham, M., and Rigby, P. W. (2014) Gene regulatory networks and transcriptional mechanisms that control myogenesis. *Dev. Cell* **28**, 225–238
12. Shirakawa, T., Toyono, T., Inoue, A., Matsubara, T., Kawamoto, T., and Kokabu, S. (2022) Factors regulating or regulated by myogenic regulatory factors in skeletal muscle stem cells. *Cells* **11**, 1493
13. Lei, S., Li, C., She, Y., Zhou, S., Shi, H., and Chen, R. (2023) Roles of super enhancers and enhancer RNAs in skeletal muscle development and disease. *Cell Cycle (Georgetown, Tex.)* **22**, 495–505
14. Hernández-Hernández, O., Ávila-Avilés, R. D., and Hernández-Hernández, J. M. (2020) Chromatin landscape during skeletal muscle differentiation. *Front. Genet.* **11**, 578712
15. Lloyd, E. M., Pinniger, G. J., Murphy, R. M., and Grounds, M. D. (2023) Slow or fast: implications of myofibre type and associated differences for manifestation of neuromuscular disorders. *Acta Physiol. (Oxford, England)* **238**, e14012
16. Pinney, D. F., Pearson-White, S. H., Konieczny, S. F., Latham, K. E., and Emerson, C. P., Jr. (1988) Myogenic lineage determination and differentiation: evidence for a regulatory gene pathway. *Cell* **53**, 781–793
17. Johnson, L. L., Hebert, S., Kueppers, R. B., and McLoon, L. K. (2023) Nystagmus associated with the absence of MYOD expression across the lifespan in extraocular and limb muscles. *Invest. Ophthalmol. Vis. Sci.* **64**, 24
18. Paulissen, E., and Martin, B. L. (2022) Myogenic regulatory factors Myod and Myf5 are required for dorsal aorta formation and angiogenic sprouting. *Dev. Biol.* **490**, 134–143
19. Wei, Y. D. (2009) *Cloning of duck MyoD1 and Myf5 genes CDS sequences and research about their differential development expression in duck muscle tissues*. Ma.D. thesis, Sichuan Agricultural University
20. Bowlin, K. M., Embree, L. J., Garry, M. G., Garry, D. J., and Shi, X. (2013) Kbtbd5 is regulated by MyoD and restricted to the myogenic lineage. *Differ. Res. Biol. Divers.* **86**, 184–191
21. Yagi, M., Ji, F., Charlton, J., Cristea, S., Messemer, K., Horwitz, N., *et al.* (2021) Dissecting dual roles of MyoD during lineage conversion to mature myocytes and myogenic stem cells. *Genes Dev.* **35**, 1209–1228
22. Du, J., Shen, L., Zhang, P., Tan, Z., Cheng, X., Luo, J., *et al.* (2018) The regulation of skeletal muscle fiber-type composition by betaine is associated with NFATc1/MyoD. *J. Mol. Med. (Berlin, Germany)* **96**, 685–700
23. Chatham, J. C., Young, M. E., and Zhang, J. (2020) Reprint of: role of O-linked N-acetylglucosamine (O-GlcNAc) modification of proteins in diabetic cardiovascular complications. *Curr. Opin. Pharmacol.* **54**, 209–220
24. Silva-Aguiar, R. P., Peruchetti, D. B., Pinheiro, A. A. S., Caruso-Neves, C., and Dias, W. B. (2022) O-GlcNAcylation in renal (Patho)Physiology. *Int. J. Mol. Sci.* **23**, 11260
25. Shi, H., Munk, A., Nielsen, T. S., Daughtry, M. R., Larsson, L., Li, S., *et al.* (2018) Skeletal muscle O-GlcNAc transferase is important for muscle energy homeostasis and whole-body insulin sensitivity. *Mol. Metab.* **11**, 160–177
26. Zumbaugh, M. D., Yen, C. N., Bodmer, J. S., Shi, H., and Gerrard, D. E. (2021) Skeletal muscle O-GlcNAc transferase action on global metabolism is partially mediated through interleukin-15. *Front. Physiol.* **12**, 682052
27. Liu, Y., Xu, B., Hu, Y., Liu, P., Lian, S., Lv, H., *et al.* (2021) O-GlcNAc/Akt pathway regulates glucose metabolism and reduces apoptosis in liver of piglets with acute cold stress. *Cryobiology* **100**, 125–132
28. Huang, P., Ho, S. R., Wang, K., Roessler, B. C., Zhang, F., Hu, Y., *et al.* (2011) Muscle-specific overexpression of NCOATGK, splice variant of O-GlcNAcase, induces skeletal muscle atrophy. *Am. J. Physiol. Cell Physiol.* **300**, C456–C465
29. Ogawa, M., Mizofuchi, H., Kobayashi, Y., Tsuzuki, G., Yamamoto, M., Wada, S., *et al.* (2012) Terminal differentiation program of skeletal myogenesis is negatively regulated by O-GlcNAc glycosylation. *Biochim. Biophys. Acta* **1820**, 24–32
30. Clarke, A. J., Hurtado-Guerrero, R., Pathak, S., Schüttelkopf, A. W., Borodkin, V., Shepherd, S. M., *et al.* (2008) Structural insights into mechanism and specificity of O-GlcNAc transferase. *EMBO J.* **27**, 2780–2788
31. Feng, Q., Jagannathan, S., and Bradley, R. K. (2017) The RNA surveillance factor UPF1 represses myogenesis via its E3 ubiquitin ligase activity. *Mol. Cel.* **67**, 239–251.e236
32. He, X. F., Hu, X., Wen, G. J., Wang, Z., and Lin, W. J. (2023) O-GlcNAcylation in cancer development and immunotherapy. *Cancer Lett.* **566**, 216258
33. Liu, Y., Hu, Y. J., Fan, W. X., Quan, X., Xu, B., and Li, S. Z. (2022) O-GlcNAcylation: the underestimated emerging regulators of skeletal muscle physiology. *Cells* **11**, 1789
34. Zhang, X., Wang, L., Lak, B., Li, J., Jokitalo, E., and Wang, Y. (2018) GRASP55 senses glucose deprivation through O-GlcNAcylation to promote autophagosome-lysosome fusion. *Dev. Cell* **45**, 245–261.e246
35. Guinez, C., Lemoine, J., Michalski, J. C., and Lefebvre, T. (2004) 70-kDa-heat shock protein presents an adjustable lectinic activity towards O-linked N-acetylglucosamine. *Biochem. Biophys. Res. Commun.* **319**, 21–26
36. Sarkar, A., and Wintrode, P. L. (2011) Effects of glycosylation on the stability and flexibility of a metastable protein: the human serpin α(1)-antitrypsin. *Int. J. Mass Spectrom.* **302**, 69–75
37. Martínez-Férriz, A., Ferrando, A., Fathinajafabadi, A., and Farràs, R. (2022) Ubiquitin-mediated mechanisms of translational control. *Semin. Cel. Dev. Biol.* **132**, 146–154
38. Wang, J., Zhou, Q., Ding, J., Yin, T., Ye, P., and Zhang, Y. (2022) The conceivable functions of protein ubiquitination and deubiquitination in reproduction. *Front. Physiol.* **13**, 886261
39. Wang, X., Zhang, X., Song, C. P., Gong, Z., Yang, S., and Ding, Y. (2023) PUB25 and PUB26 dynamically modulate ICE1 stability via differential ubiquitination during cold stress in Arabidopsis. *Plant cell* **35**, 3585–3603

40. Zhang, M., Zhou, W., Cao, Y., Kou, L., Liu, C., Li, X., *et al.* (2024) O-GlcNAcylation regulates long-chain fatty acid metabolism by inhibiting ACOX1 ubiquitination-dependent degradation. *Int. J. Biol. Macromol.* **266**, 131151
41. Stuelsatz, P., Pouzoulet, F., Lamarre, Y., Dargelos, E., Poussard, S., Leibovitch, S., *et al.* (2010) Down-regulation of MyoD by calpain 3 promotes generation of reserve cells in C2C12 myoblasts. *J. Biol. Chem.* **285**, 12670–12683
42. Goljanek-Whysall, K., Pais, H., Rathjen, T., Sweetman, D., Dalmay, T., and Münsterberg, A. (2012) Regulation of multiple target genes by miR-1 and miR-206 is pivotal for C2C12 myoblast differentiation. *J. Cel. Sci.* **125**, 3590–3600